Hydrogenation of 1,5,9-cyclododecatriene in fixed-bed reactors: Down- vs. upflow modes

Raghunath Vitthal Chaudhari, Rengaswamy Jaganathan, Suju P. Mathew, Carine Julcour-Lebigue, Henri Delmas

Hydrogenation of 1,5,9 Cyclododecatriene in Fixed Bed Reactors: Down- vs Upflow Modes

R. V. Chaudhari*, R. Jaganathan and S. P. Mathew
National Chemical Laboratory, Pune 411 008, India

C. Julcour and H. Delmas
ENSIGC, 18, Chemin de la Loge - 31078 Toulouse Cedex 4, France

Abstract

Performance of trickle-bed and upflow reactors was studied experimentally and theoretically for an exothermic multistep hydrogenation of 1,5,9-cyclododecatriene (CDT) in n-decane as solvent over 0.5% Pd/alumina catalyst. Intrinsic kinetics was studied in a batch stirred slurry reactor using the powdered catalyst and a Langmuir-Hinshelwood type rate model is proposed. Using this rate equation, a trickle-bed-reactor model was developed which incorporates contributions of partial wetting and stagnant liquid holdup, in addition to the external and intraparticle mass transfer for the gas-phase reactant (hydrogen). It was also modified to describe the behavior of the upflow reactor. Experimental data were obtained in both upflow and downflow modes at different liquid velocities, pressures and inlet feed concentrations at 373-413 K. Reactor performance of the two modes was compared in terms of global hydrogenation rate, CDT conversion, selectivity to cyclododecene and the maximum temperature rise observed in the catalyst bed. The conversions and the global hydrogenation rate were significantly higher in a trickle- bed reactor than in the upflow reactor. Similarly, a significant temperature rise in the catalyst bed was observed for the downflow operation compared to the u-flow mode, which is explained from wetting characteristics of the catalyst bed. Model predictions for both reactors agreed well with experimental data.

Key words: Fixed bed, upflow, downflow, catalytic hydrogenation, reactor modeling.

Introduction

Multiphase catalytic reactors have wide-ranging applications in the chemical industry in a variety of processes in which reactions of gas- and liquid-phase reactants in the presence of solid catalysts are involved. Some important examples are: hydro processing of petroleum feed stocks, hydrogenation of organic compounds for fine chemicals and pharmaceuticals, oxidation, hydration [Ramachandran and Chaudhari (1983), Mills and Chaudhari (1997)]. Among the industrial reactors, trickle-bed reactors with down-flow of gas and liquid phases are the most commonly used reactor types, as they are in large-scale processes for hydroprocessing and petrochemicals [Trambouze (1991)]. Due to increasing competition and environmental needs, however, alternative modes of operation, such as fixed-bed with upflow of gas and liquid phases are, also gaining considerable attention [Dassori (1998)]. The upflow mode may have advantages with respect to uniform liquid distribution, reliable scale-up, selectivity, temperature control and removal of inhibitory byproducts. Therefore, systematic theoretical and experimental studies on comparison of the reactor performances for downflow (trickle-bed) and upflow modes are most essential.

The analysis of trickle-bed reactors incorporating the contributions of reaction kinetics, external and intraparticle mass transfer, and wetting characteristics of catalyst particles have been extensively studied including experimental verification of the reactor models [Rajashekharam et al. (1998), Khadilkar et al. (1996, 1998), Bergault et al. (1997)]. The current state of development on this subject has been reviewed by Al-Dahhan et al. (1997) and Dudukovic et al. (1999). In most cases, the plug-flow models with partial wetting of catalyst particles were found to be representative for trickle-bed reactors at lower liquid velocities. The effect of evaporating solvents [Van Gelder et al. (1990)], and other models based on liquid-flow maldistribution, stagnant liquid pockets in the reactor [Rajashekharam et al. (1998)] and mixing cell model [Brahme et al. (1984), Jaganathan et al. (1987)] have also been considered. Most of the previous studies on reactor performance have considered single reactions, with a few exceptions wherein complex multistep reactions have been considered under isothermal conditions. An important issue in the design and scale-up of fixed-bed multiphase reactors is the control of temperature, which requires a detailed analysis of nonisothermal effects. In only a few

cases have the reactor modeling and experimental verification under nonisothermal conditions been considered in a trickle-bed reactor [Hanika et al. (1977), Rajashekharam et al. (1998), Bergault et al. (1997), Julcour et al. (2000)].

The upflow reactor has the advantage of completely wetted catalysts, thus providing better mass transfer and heat transfer between the liquid phase and the solid catalyst. But it has the disadvantage of significant external mass-transfer resistance. Al-Dahhan and Dudukovic (1996) and Wu et al. (1996) have shown that under conditions of liquid-phase reactant limitation, the upflow reactor outperforms the trickle-bed reactor due to its efficient liquid-solid contact. The higher liquid holdup and effective liquid-solid contact also results in a better heat dissipation in the case of exothermic reactions and can be advantageous in reactions where temperature dependence of selectivity is sensitive. Reactor performance studies in upflow reactors for hydrogenation reactions are rare compared to trickle-bed reactor studies [Mochizuki and Matsui (1976), Herrmann and Emig (1998) and Stuber et al. (1995)] and most of these studies were carried out under isothermal conditions. Nonisothermal reactor performance and theoretical model prediction for upflow reactors are scarce in literature. Van Gelder et al. (1990 a, b) have described a reactor model for the hydrogenation of 2,4,6-trinitrotoluene in an upflow reactor in the presence of an evaporating solvent to absorb the heat of reaction. They have shown that a model incorporating dispersion of gas phase represents the experimental data better compared to a plug-flow model.

Comparison of the performance for up- and downflow fixed-bed multiphase reactors is necessary to understand clearly the distinguishing features of these two modes. In the previous work, studies on comparison of up- and downflow modes involving both theoretical and experimental aspects have been reported for single reactions under isothermal conditions [de Wind et al. (1988), Goto et al. (1984), Mills et al. (1984), Leung et al. (1986), Wu et al. (1996), Khadilkar et al. (1996)]. Some important findings are summarized in Table 1. Comparison of reactor performance under nonisothermal conditions has not been investigated in detail. In a recent report, Julcour et al. (2000) investigated the hydrogenation of 1,5,9-cyclododecatriene (CDT) and observed that the rate of hydrogenation was higher for the upflow mode compared to downflow, in contrast to earlier reports. However, a detailed experimental study on the effect of different

parameters under nonisothermal conditions has not been published. The aim of this paper is to present a systematic study on the comparison of a fixed-bed reactor in the downflow and upflow modes operated under nonisothermal conditions for the hydrogenation of 1,5,9-CDT using 0.5% palladium on alumina catalyst. Experiments have been carried out over a wide range of operating conditions for both the downflow and upflow modes of operations. For predicting the trickle-bed reactor performance, a nonisothermal plug-flow model taking into consideration the external and intraparticle mass-transfer resistance of gas-phase reactant (hydrogen) and the wetting characteristics of the catalyst pellets have been developed. For the upflow reactor, the trickle-bed reactor model has been modified suitably. The effect of liquid flow rate, pressure and inlet substrate concentration on the performance under the two modes of operation have been studied in the temperature range 373 - 433 K and model predictions compared with experimental data.

Experimental

Materials

1,5,9-CDT and the catalyst were procured from M/s. Aldrich Chemicals (USA). The catalyst used was 0.5% Pd/Alumina pellets, with an average particle size of 3 $x10^{-3}$ m. The solvent used was n-decane and was procured from M/s. S.D. Fine Chemicals (India).

Kinetic Experiments

For evaluation of intrinsic kinetics, the catalyst pellets were crushed to a fine powder (< 50 microns) and the hydrogenation experiments were carried out in a 300 ml capacity autoclave (Parr Instruments, USA), a detailed description of which is given elsewhere [Jaganathan et. al. (1999)]. In a typical experiment, a known amount of catalyst along with 100 ml of CDT solution of known concentration in n-decane was charged in the reactor and the contents flushed with nitrogen at room temperature. The heating was then started, and after the desired temperature was reached, the system was pressurised with hydrogen to the desired pressure and the reaction was started by

switching the stirrer on. Samples were taken at frequent intervals and analysed for the reactants and products.

Fixed Bed Reactor Experiments

The experiments were carried out in a trickle-bed reactor procured from M/s. "Vinci Technologies", France. The schematic of the reactor setup is shown in Figure 1. The reactor consists of a stainless steel tube of 0.53 m in length and 1.9 x 10^{-2} m, inner diameter. The reactor was also provided with three thermocouples [Chromel-Alumel, type K] to measure temperatures at three different points, namely, along the length of the reactor. A thermo well made of stainless steel of outer diameter 0.8 x 10^{-2} m placed axially along the reactor length had the thermocouples in it. An electronically controlled furnace split into three separate sections heated the reactor, and the corresponding wall temperatures could also be noted from the electronic display along with that of the reactor bed temperature. The temperature of each of these furnaces could be controlled independently. The gas flow rate was adjusted by a mass-flow controller with a range of 0-60 Nl/h and could be read from the electronic display. The reactor pressure was adjusted with the manual pressure controller and the pressure was indicated by the pressure gauge fitted at the reactor inlet. For quick pressurization of the unit, the mass-flow controller can be bypassed by a manually operated valve. A storage tank with the liquid feed was kept on a weighing balance with an accuracy of 0.5 g and the exact flow rate of liquid feed was calculated from the weight drop observed from the weighing balance. The pump had a maximum capacity of 2.5 x10^{-3} m^3/h. The outlet of the reactor was equipped with a condenser and a high-pressure gas-liquid separator, and a liquid-level indicator. The gas outlet line was equipped with a back-pressure controller, which maintained a constant pressure in the unit by continuous pressure release. A wet gas flowmeter measured the total gas outflow. The liquid product from the gas-liquid separator could be drained by means of a “block and bleed valve”. In each experiment, the required amount of catalyst was charged in the reactor, and the sections above and below the catalyst bed were packed with inert packing (carborundum). The lines of the reactor were flushed with the feed solution before the start of any experiment. In the beginning, the reactor was flushed with nitrogen well and the wall temperatures of the

different zones were set to the desired limit. The liquid flow was started after adjusting the required flow rate. Once the temperature of the wall was attained and the temperature inside the reactor was stable, the reactor was pressurized after setting the gas flow rate. Liquid samples were withdrawn from the exit at regular intervals of time and were analysed by gas chromatography. The temperatures inside the reactor were monitored at three positions inside the reactor. The catalyst was filled in such a way that the first thermocouple was at the inlet of the catalyst bed, the second one was at the middle of the catalyst bed, and the third thermocouple was at the exit of the catalyst bed. Following this procedure, experiments were carried out at different inlet conditions and steady-state performance of the reactor observed by analysis of reactants and products in the exit streams. In all the experiments steady state was reached in about 15 min.

Analysis

Liquid samples were analysed by gas chromatography (model HP-19091F-102) using a HP-FFAP PEG TPA Capillary column of 25 m x 200 μm x 0.30 μm. The other conditions of the GC were: injector temperature: 200^{o}C; column temperature: 110 to 140^{o}C programmed at 4^{o}C / min; detector (FID) temperature: 250^{o}C.

Many isomers are formed in the hydrogenation of 1,5,9-CDT. The substrate 1,5,9-CDT used in this work itself contained three isomers, 97% cis,trans,trans (ctt), 2% trans,trans,trans (ttt) and 0.5 % cis,cis,cis (ccc). Stuber et al. (1995) have reported at least 14 different isomers by GC-NMR analysis.

Reactor model

Intrinsic Kinetics

In order to develop rate equations for the different steps in hydrogenation of 1,5,9 cyclododecatriene using 0.5% Pd/alumina catalyst, experiments were carried out in a batch slurry reactor using the powdered catalyst and n-decane as a solvent. Though the kinetics of this reaction has been investigated before [Benaissa et al., (1996), Stuber et al. (1995)] using pure CDT as the feedstock and 0.5% Pd/alumina (supplied by Degussa, Germany), it was thought necessary to determine the kinetic parameters for the specific

catalyst (0.5% Pd/Alumina supplied by Aldrich, USA) and solvent (n-decane) used in this study. A number of isomers of intermediate products are formed during the hydrogenation, but the main products are: cyclododecadiene (CDD), cyclododecene (CDE) and cyclododecane (CDA). The different isomers observed include four CDT, three CDD and two CDE isomers. Furthermore, two CDT and three CDD positional isomers were also found, though the concentration of these positional isomers was negligible. In this work, a lumped reaction scheme was considered as shown below for kinetic modelling:

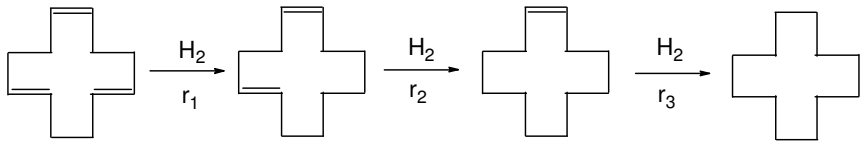

CDT **CDD** **CDE** **CDA**

Experiments were carried at different catalyst loadings, hydrogen partial pressures and initial CDT concentrations in a temperature range of 353 to 398 K, in which concentration-time data were obtained. The procedure followed for kinetic modeling was similar to that discussed earlier [Benaissa et al. (1996)]. Langmuir-Hinshelwood type of rate equations given below were found to represent the data satisfactorily, as evidenced by the comparison between the experimental and predicted results shown in Figure 2 for 353 and 373 K.

$$r_1 = \frac{wk_1 BA^*}{(1 + K_B B + K_c C + K_E E)} \tag{1}$$

$$r_2 = \frac{wk_2 CA^*}{(1 + K_B B + K_c C + K_E E)} \tag{2}$$

$$r_3 = \frac{wk_3 EA^*}{(1 + K_B B + K_c C + K_E E)} \tag{3}$$

Where A* represents the dissolved hydrogen concentration in equilibrium with the gas phase, kmol/m^3 and B, C and E represent concentrations of cyclododecatriene (CDT) cyclododecadiene (CDD) and cyclododecene (CDE), respectively in kmol/m^3. The rate parameters evaluated for Eqs. (1) to (3) are presented in Table 2. The activation energies for the reaction steps r_1, r_2 and r_3 were found to be 41, 41 and 35 kJ/mol, respectively. The activation energies for the constants K_B, K_C, and K_E were 14.8, 15.21 and 15.0 kJ/mol, respectively.

The activation energies are somewhat low, which may indicate transport limitations. However, we have ensured by well-known criteria involving the comparison of the rate of hydrogenation with the maximum rate of gas-liquid, liquid-solid, and intraparticle diffusion rates, that mass-transfer resistances were unimportant under the conditions of kinetic study [Jaganathan et al. (1999), Rajashekharam et al. (1997)].

Trickle-bed Reactor Model

A trickle bed reactor model for hydrogenation of CDT was developed similar to that proposed earlier [Rajasekheram et al. (1998)]. The salient features of the model are: the spherical catalyst particle was assumed to be divided into three zones which represented (i) a dry zone, (ii) a wetted zone covered by the flowing dynamic liquid and (iii) a wetted zone covered by the stagnant liquid. It was assumed that (a) gas and liquid phases are in plug flow; (b) liquid-phase reactant is non-volatile and is in excess compared to the gaseous reactant concentration in the liquid phase; (c) the gas-liquid, liquid-solid and intraparticle mass-transfer resistances for H_2 are considered, whereas the liquid-solid and intraparticle mass transfer resistances for the liquid-hase components are assumed to be negligible; (d) the interphase and intraparticle heat-transfer resistances are negligible, but bed-to-wall heat transfer has been considered to incorporate the non-isothermal effects; (e) the overall catalytic effectiveness factor can be expressed as a sum of the weighted average of the effectiveness factors in the dynamic liquid-covered, stagnant-liquid-covered and gas-covered zones, respectively, that is,

$$\eta = f_d\eta_d + f_s\eta_s + (1 - f_d - f_s)\eta_g \qquad (4)$$

where η is the overall catalytic effectiveness factor under conditions of partial wetting and stagnant liquid pockets, and f_d and f_s are the fractions of catalyst particle covered by the dynamic and stagnant-liquid zones; and η_d, η_s and η_g are the overall effectiveness factors for dynamic, stagnant and dry zones, respectively. For conditions of complete wetting and absence of stagnant-liquid pockets $\eta = \eta_c$.

The catalytic effectiveness factor equations applicable to hydrogenation of CDT were developed following the well-known approaches [Bischoff (1965); Ramachandran and Chaudhari (1983)]. Under the conditions of significant intraparticle gradients for the gas-phase reactant (H_2) and when the liquid-phase reactant is in excess, the overall rate of hydrogenation can be expressed as (combining Eqs. (1)-(3))

$$R_A = \frac{\eta\, w\, (k_1 B_l + k_2 C_l + k_3 E_l) A^*}{(1 + K_B B_l + K_c C_l + K_E E_l)} \tag{5}$$

where η is given by Eq. (4) and η_c is given by the following expression for a spherical catalyst particle:

$$\eta_c = \frac{1}{\phi}\left(\coth 3\phi - \frac{1}{3\phi}\right) \tag{6}$$

where ϕ is the Thiele parameter defined as:

$$\phi = \frac{R}{3}\left[\frac{S_p (k_1 B_l + k_2 C_l + k_3 E_l)}{D_e (1 + K_B B_l + K_C C_l + K_E E_l)}\right]^{1/2} \tag{7}$$

or in dimensionless form as:

$$\phi = \phi_0\left[\frac{(b_l + k_{21} c_l + k_{31} e_l)}{(1 + k_b b_l + k_c c_l + k_e e_l)}\right]^{1/2} \tag{8}$$

$$\phi_0 = \frac{R}{3}\left[\frac{\rho_p k_1 B_{l_i}}{D_e}\right]^{1/2} \tag{9}$$

The dimensionless mass balance equations for the different species involved in the reaction are given below. (The detailed derivation is followed from our earlier paper, [Rajashekharm et al. (1998)]. The dimensionless mass balance equation for species A (hydrogen) is:

$$-\frac{da_{l_d}}{dz} + \alpha_{gl}(1-a_{l_d}) = \frac{\eta_c \alpha_r (b_1 + k_{21}c_1 + k_{31}e_1)}{(1+k_b b_1 + k_c c_1 + k_e e_1)} \times \left\{ \frac{f_d a_{l_d}}{(1+\eta_c \phi^2 / N_d)} + \frac{f_s a_{l_d}}{(1+\eta_c \phi^2 / N_s) + (\eta_c \phi^2 / \alpha_s N_s)} \right\} \tag{10}$$

with

$$(1-f_d-f_s)\alpha_{gs}(1-a_{s_g}) = (1-f_d-f_s) \times \frac{\eta_c \alpha_r (b_1 + k_{21}c_1 + k_{31}e_1)}{(1+k_b b_1 + k_c c_1 + k_e e_1)} \times \left[\frac{1}{(1+\eta_c \phi^2 / N_g)} \right] \tag{11}$$

The mass balances of liquid-phase reactants/products in dimensionless form are given as:

$$-\frac{db_{l_d}}{dz} = \frac{\eta_c \, \alpha_r \, b_1 \, \chi}{q_B (1 + k_b b_1 + k_c c_1 + k_e e_1)} \tag{12}$$

$$\frac{dc_{l_d}}{dz} = \frac{\eta_c \alpha_r (b_1 - k_{21} c_1) \chi}{q_B (1 + k_b b_1 + k_c c_1 + k_e e_1)} \tag{13}$$

$$\frac{de_{l_d}}{dz} = \frac{\eta_c \alpha_r (k_{21} c_1 - k_{31} e_1) \chi}{q_B (1 + k_b b_1 + k_c c_1 + k_e e_1)} \tag{14}$$

$$\frac{dp_{l_d}}{dz} = \frac{\eta_c \alpha_r k_{31} e_1 \chi}{q_B (1 + k_b b_1 + k_c c_1 + k_e e_1)} \tag{15}$$

$$\text{with } \chi = \left\{ \frac{f_d \, a_{l_d}}{(1+\eta_c \phi^2 / N_d)} + \left[\frac{f_s \, a_{l_d}}{(1+\eta_c \phi^2 / N_s) + (\eta_c \phi^2 / \alpha_s N_s)} \right] + \frac{(1-f_d-f_s)}{(1+\eta_c \phi^2 / N_g)} \right\} \tag{16}$$

The dimensionless parameters used in the above equations are defined in Table 3. In deriving a nonisothermal trickle-bed reactor model, the dependencies of various parameters like, reaction rate constants, equilibrium constants, effective diffusivity and saturation solubility on temperature are accounted for. The effective diffusivity was calculated as

$$D_e(T_o) = D_m \frac{\varepsilon}{\tau} \tag{17}$$

where D_m is the molecular diffusivity and is evaluated from the correlation of Wilke and Chang (1955), ε and τ represent the porosity and the tortuosity factors. The porosity and tortuosity values were taken as 0.45 and 7.2 respectively [Stuber et al. (1995)]. The variation of the vapor pressure with temperature for solvent n-decane was calculated from the following equations reported in the literature [Stephan and Stephan (1963)]

$$\log(P_V)_T = \frac{0.2185 \times 10912}{T} + 8.24889 \tag{18}$$

Since, dilute solutions of CDT were used in the present study, the vapor pressure of CDT was neglected in the calculations. The solubility of hydrogen in CDT - n-decane mixture was determined experimentally and the Henry's constant of solubility, H_e, was expressed by the following correlation.

$$(H_e)_T = -1.9\,x10^{-3} + 1.82\,x10^{-5}\ T\ - 1.89\,x10^{-5}\ Y \tag{19}$$

Where T is the temperature, Y the concentration of CDT in % (w/w) and $(H_e)_T$ the Henry's constant expressed as kmol/m^3/atm.

The heat evolved during the reaction was assumed to be carried away by the flowing liquid and transfer to the reactor wall, which is characterized by the bed-to-wall heat transfer coefficient, U_W. Under such conditions, where the interphase and intraparticle heat-transfer resistances are assumed to be negligible, the heat balance of the

reactor can be expressed in dimensionless form as [Ramachandran and Chaudhari (1983)]:

$$\frac{d\theta}{dz} = \frac{\eta_c \alpha_r \beta_1 (b_1 + k_{21} c_1 + k_{31} e_1)\chi}{q_B (1 + k_B b_1 + k_C c_1 + k_E e_1)} - \beta_2 (\theta_b - \theta_W) \tag{20}$$

Where β_1 is the thermicity parameter and other dimensionless parameters are given in Table 3. Eqs. (10) to (15) combined with Eq. (19) were solved using a fourth-order Runge-Kutta method to predict the concentrations of reactants/products and the temperature along the length of the reactor with the following initial conditions:

$$\text{at } z = 0; \quad a_1 = b_1 = 1; \quad c_1 = e_1 = p_1 = 0; \quad \theta = 1 \tag{21}$$

From these results, the conversion of CDT (X_B) was calculated as:

$$X_B = 1 - b_1 \tag{22}$$

The global rate of hydrogenation (including hydrogen consumption in all the steps) was calculated as:

$$R_A = \frac{U_l}{L}(C_1 + 2E_1 + 3P_1) \tag{23}$$

Where U_l is the liquid velocity in m/s, L is the length of the catalyst bed in m, C_1, E_1, P_1 are the concentrations of CDD, CDE and CDA, respectively, at the exit of the reactor, kmol/m^3. The model parameters were evaluated using correlations given in Table 4.

Model for Upflow Reactor

The model equations described above for the downflow reactor can also be used for the upflow reactor with appropriate modifications and relevant parameters. Since the catalyst is completed wetted in the upflow operation, the wetting efficiency was taken as unity. The correlations used for evaluation of hydrodynamics and mass-transfer parameters for the upflow mode are presented in Table 5.

For the simulation of experimental data with model predictions, we have used literature correlations except for the bed-to-wall heat-transfer coefficient, for which reliable correlations are not available. The strategy followed was to fit this parameter (bed-to-wall heat-transfer coefficient) using one or two sets of experimental data at different gas and liquid velocities. These parameters were then used at appropriate gas and liquid velocities for simulation of results under a wide range of conditions.

Results and discussion

Experimental data were obtained for both trickle-bed (downflow) and upflow modes of operation in which liquid velocity, pressure of hydrogen, inlet concentration of CDT and temperature were varied. In the following sections, the effect of these parameters on the overall rate of hydrogenation, conversion of CDT and temperature rise is discussed. The results have been compared with model predictions for each mode of operation, and the reactor performance for the two modes is also compared based on experimental data obtained under identical conditions.

Trickle-bed Reactor Performance

Effect of Liquid Velocity

The effect of liquid velocity on the global rate of hydrogenation, temperature rise and CDT conversion is shown in Figures 3-5. The global rate of hydrogenation and CDT conversion was found to decrease with increase in liquid velocity. Similarly, the temperature rise decreased with increase in liquid velocity at all the inlet temperatures studied (Figure 5). With increase in liquid velocity, one expects increase in wetted fraction of the catalyst as well as increase in the gas-liquid and liquid-solid mass transfer coefficients. At lower liquid velocity, catalyst particles are partially wetted and under these conditions, it is well known that the rate increases due to direct transfer of the gas-phase reactant to the catalyst surface (already wetted internally due to capillary forces). Hence, with increase in liquid velocity, increase in wetted fraction is expected to retard the rate of reaction, while an increase in the external mass-transfer coefficients will enhance, the rate resulting in opposite effects. Superimposed on these effects would be the effect of an increase in bed temperature due to exothermicity. At 373 K, wherein the

temperature rise over the entire varied liquid velocity range is less than 10 K, the liquid velocity effect is not very significant, perhaps due to the compensation of the effect of wetting and the increase in external mass-transfer coefficients. But at higher inlet temperature, 413 K, the rate decreases sharply with liquid velocity due to large difference in the temperature rise. With the increase in liquid velocity, the heat evolved due to exothermicity is removed at a significantly higher rate, resulting in reduced bed temperature rise and rate of reaction. For example, at $U_l = 5 \times 10^{-4}$ m/s, ΔT was observed as 45 K, while at $U_l = 2.1 \times 10^{-3}$ m/s, ΔT was 6 K. Thus, the trickle bed reactor performance under nonisothermal conditions is significantly different from that under isothermal conditions.

In order to compare the experimental data with model predictions, Eqs. (10) to (15) and (20), with the initial condition in Eq. (21), were solved numerically to obtain exit concentrations of all the reactants, intermediates and products, as well as the temperature along the axis for the conditions used in experiments. From these data, the conversion of CDT (X_B), the global rate of hydrogenation (R_A) and the temperature rise (ΔT) along the length of the reactor for a given set of input conditions were calculated. Besides the kinetic parameters (Table 2), other key parameters in the model for non-isothermal trickle bed reactor (downflow operation) are: wetted fraction of the catalyst particles, gas-liquid mass transfer, gas-particle mass transfer (to the unwetted portion of the catalyst) coefficient, liquid-solid mass transfer coefficients for the dynamic and stagnant liquid covered zones, effective diffusivity, and overall heat transfer coefficient. For comparison of the experiments with model predictions, temperature rise was calculated based on the temperature at z = 0.5 where the temperature in the bed could be measured. A comparison of the model predictions with experimental data is also shown in Figures 3-5 for 373, 393, 413 K, which shows excellent agreement.

Effect of Inlet CDT Concentration

The effect of CDT concentration in the inlet on global rate of hydrogenation, conversion of CDT and maximum temperature rise is shown in Figures 6 to 8 for different temperatures. The conversion of CDT was found to decrease with increase in CDT concentration, as expected, while the global rate of hydrogenation and temperature

rise were found to increase with CDT concentration. The effect of CDT concentration on the rate and ΔT was found to be significant at higher inlet temperature. At a higher inlet feed temperature (413 K), a temperature rise as high as 65 K was observed, while at a lower inlet temperature (373 K), it was only about 10 K. A comparison of these experimental data with model predictions (Figures 6-8) shows good agreement.

Effect of Hydrogen Pressure

The effect of hydrogen pressure on the global rate of hydrogenation and ΔT is shown in Figure 9 along with model predictions. Here again a good agreement between the experiments and the model prediction was observed, indicating the applicability of the model over a wide range of conditions. As expected, the rate as well as the temperature rise were found to increase with increase in pressure. At higher operating pressures the temperature rise in the catalyst bed and the global rate of hydrogenation increased nearly in a linear manner (Figure 9).

Comparison of Trickle-bed with Upflow Mode

Experiments were also carried out on hydrogenation of CDT in a fixed-bed reactor with upflow of liquid and gas at different liquid velocities, inlet temperatures, CDT concentrations and hydrogen pressures. The results, along with comparison of the data for trickle bed (downflow) under identical conditions, are discussed below.

Effect of Liquid Velocity

The effect of liquid velocity on the global rate of hydrogenation was marginal for both upflow and downflow operations at 373 K inlet temperature, though the rate was significantly higher in a trickle-bed reactor at 413 K (Figure 10). In a trickle-bed reactor, the rate decreased by 20%, but in the upflow mode, it increased by only 6% with a 4-fold increase in U_l. In the upflow mode, catalyst particles are completely covered by liquid, whereas in the trickle bed, a significant partial wetting exists in the varied range of U_l. The higher rate for the trickle bed is due to the direct mass transfer of gas-phase reactant to the catalyst surface, eliminating gas-liquid and liquid-solid mass transfer resistance. Since the rate of gas-particle mass-transfer rate is generally higher than the other steps, a significant rate enhancement is expected. In the previous work, Julcour et al. (2000) observed that the rate was higher for the upflow mode compared to trickle bed for the

same reaction system in contrast to the observations made here. However, these two studies have led to different results mainly because, in the previous work a diluted catalyst bed (100 g of catalyst mixed with 500 g of inert) was used in a pilot-scale reactor of about one-liter capacity, while for the present work an undiluted catalyst bed was used in a smaller bench-scale reactor of 100-cm^3 capacity. Indeed, the present work allowed us to consider the analysis of some differences due to scale-up operation and the dilution of the catalyst bed. The most significant effect of the dilution of the catalyst bed is on the wetting efficiency and misdistribution of liquid flowing in the trickle-bed reactor, and the different trends observed in the results in these two studies is a result of the differences in the hydrodynamic conditions due to bed dilution. The effect of the liquid velocity on the conversion of CDT and rise in temperature are shown in Figures 11 and 12. In the trickle-bed reactor, higher conversion and a higher rise in temperature was observed, but for the upflow mode, the rise in temperature was much lower due to efficient heat removal.

Effect of Pressure, Temperature and Inlet CDT Concentration

The effect of hydrogen pressure and inlet temperature on the reactor performance is shown in Figures 13 and 14 and Figures 15 and 16, respectively, for the downflow and upflow modes. The effect of inlet CDT concentration is shown in Figures 17 and 18. In all the cases, the global reaction rate and temperature rise were higher for the downflow compared to upflow. This difference is mainly due to the partial wetting of catalyst particles in downflow mode, which is known to enhance the overall rate, as discussed earlier. The observation of lower rise in temperature in the upflow mode is due to more efficient heat removal, which can be advantageous in temperature control for exothermic reactions. The experimental data over a wide range of conditions were found to agree well with model predictions for both the modes.

Selectivity Behavior

A comparison of selectivity of CDE in the two reactor modes is shown in Figures 19 to 22 for different liquid velocities, hydrogen pressure, inlet CDT concentration and inlet temperature. In general, the selectivity of CDE compared to other products (CDD and CDA) was found to be higher in trickle-bed reactor for all conditions. The selectivity

of CDE is expected to be proportional to the global rate of hydrogenation rather than CDT conversion, and since in most conditions the global rate was higher in the trickle bed, the CDE selectivity was also higher. In the previous work [Julcour et al. (2000)], the global rate was higher for the upflow operation compared to trickle bed and the selectivity of CDE defined, as the ratio of [(CDE / (CDE+CDA)) x100] was also higher for the upflow mode. For the present work, the selectivity defined as [(CDE / (CDE+CDA)) x100] was higher for upflow, as was that observed by Julcour et al. (2000); however, the selectivity in relation to all the products [(CDE / (CDD+CDE+CDA)) x100] was found to be higher in downflow mode. This is due to significant formation of CDA in the trickle bed compared to upflow mode.

Conclusions

The hydrogenation of 1,5,9-cyclododecatriene using 0.5% Palladium on Alumina as the catalyst was investigated in a trickle bed (downflow) as well as upflow mode under nonisothermal conditions. The effect of liquid velocity, hydrogen pressure, and inlet CDT concentration on the global rate of hydrogenation, CDT conversion, temperature rise and CDE selectivity was studied in a temperature (inlet) range of 373 - 413 K. Theoretical models for the trickle bed and upflow modes have been developed incorporating the contributions of external and intraparticle mass transfer, partial wetting of catalyst (for downflow), overall heat transfer and complex reaction kinetics applicable to hydrogenation of CDT. The experimental data over a wide range of conditions were found to agree well with model predictions for both the modes.

The comparison of the reactor performance in the two modes indicated that (i) trickle bed (downflow) gives higher rate of reaction as a result of partial wetting phenomena. Comparison of the results with previous work indicated that for diluted catalyst beds, the performance of upflow mode is higher than trickle bed due to poor utilization of catalyst in downflow mode as a result of channeling of liquid flow and inefficient external as well as internal wetting of catalyst, (ii) the temperature rise is lower for the upflow mode, which also results in lower rate, but can be a useful tool for temperature control, and (iii) the selectivity of CDE in relation to CDA was higher in

upflow mode, but when compared with all the products formed, it was higher in the downflow mode. The selectivity behavior at different conditions observed experimentally was also found to agree with the model predictions.

Acknowledgments

The authors would wish to thank IFCPAR (Indo-French Center for the Promotion of Advanced Research) for the financial support of this work. One of the authors S. P. Mathew wishes to thank Council of Scientific and Industrial Research (CSIR), India, for providing him a research fellowship.

Notations

a_B gas-liquid interfacial area, m^2/m^3

a_l dimensionless concentration of hydrogen in liquid phase, (A_l / A^*)

a_s dimensionless concentration of hydrogen on the catalyst surface, (A_s / A^*)

a_p external surface area of the pellet, $[6 (1-\varepsilon_B) / d_p]$, m^{-1}

a_t packing external surface area of the per unit volume of reactor $[S_{ex} (1-\varepsilon_B) / V_B]$, m^{-1}

a_w catalyst area wetted, m^{-1}

A_l concentration of hydrogen in liquid phase, $kmol/m^3$

A_s concentration of hydrogen on the catalyst surface, $kmol/m^3$

A^* concentration of hydrogen in equilibrium, $kmol/m^3$

b_l dimensionless concentration of CDT in liquid phase, (B_l / B_{li})

B_l concentration of CDT in liquid phase, $kmol/m^3$

B_{li} initial concentration of CDT in liquid phase, $kmol/m^3$

c_l dimensionless concentration of CDD in liquid phase, (C_l / B_{li})

C_l concentration of CDD in liquid phase, $kmol/m^3$

C_{pl} heat capacity of liquid, kJ/K/kg

C_{pg} heat capacity of gas, kJ/K/kg

D_e effective diffusivity, m^2/s

D_m molecular diffusivity, m^2/s

d_p particle diameter, m

d_T reactor diameter, m

e_l dimensionless concentration of CDE in liquid phase, (E_l / B_{li})

E_l concentration of CDE in liquid phase, $kmol/m^3$

E_i activation energy for hydrogenation step i, kJ/mol

f_d fraction of catalyst wetted by the dynamic liquid

f_s fraction of catalyst wetted by the stagnant liquid

f_w wetted fraction

H_e Henry's constant of solubility, $kmol/m^3/atm$

h_w overall heat transfer coefficient, $kJ/m^2/K/s$

k_1 to k_3 reaction rate constants, $(m^3/kg)\ (m^3/kmol)\ s^{-1}$

k_{21} dimensionless rate constant (k_2 / k_1)

k_{31} dimensionless rate constant (k_3 / k_1)

k_b, k_c, k_e dimensionless equilibrium constants

$(k_b = K_B B_{li}\ ;\ k_c = K_C B_{li}\ ;\ k_e = K_E B_{li}\ )$

k_s liquid-solid mass transfer coefficient, $m\ s^{-1}$

k_{gs} gas-particle mass transfer coefficient, $m\ s^{-1}$

K_B, K_C, K_E equilibrium constants, $m^3/kmol$

$k_l a_B$ gas-liquid mass transfer coefficient, s^{-1}

k_{ex} exchange coefficient between dynamic and stagnant liquid, s^{-1}

L reactor length, m

L_m superficial liquid mass velocity, $kg/m^2/s$

N_d Nusselt number for liquid phase in the dynamic zone

N_s Nusselt number for liquid phase in the stagnant zone

N_g Nusselt number for gas phase

p_l dimensionless concentration of CDA in liquid phase (P_l / B_{li})

P_l concentration of CDA in liquid phase, $kmol/m^3$

Pr Prandtl number of liquid phase $(C_{pl}\mu_l / \lambda_{eff})$

P_V vapor pressure of solvent, mmHg (as defined by Eq. (18))

q_B stoichiometric ratio (B_{li} / A^*)

r_1 to r_3 reaction rate for individual hydrogenation steps, kmol/m^3/s

R radius of the pellet, m

R_A global rate of hydrogenation, kmol/m^3/s

R_g universal gas constant, kJ/kmol/K

Re_l Reynolds number for liquid phase

S_{ex} external surface area of the catalyst pellet, m^2

T_o inlet temperature, K

T_b bed temperature, K

T_W wall temperature, K

U_g gas velocity, m/s

U_l liquid velocity, m/s

U_W bed-to-wall heat transfer coefficient, kJ/m^2/K/s

V_R reactor volume, m^3

w catalyst loading, kg/m^3

We_l weber number for liquid (L_m^2 / $\sigma_l \rho_l a_t$)

z dimensionless reactor length

Greek letters

α_{gl} dimensionless gas-liquid mass-transfer coefficient

α_{ls} dimensionless liquid-solid mass-transfer coefficient

α_r dimensionless reaction rate constant

α_s dimensionless exchange coefficient

β_1 themicity parameter

β_2 dimensionless heat-transfer parameter

δ_{gl} two phase pressure drop, N/m^2

ΔH heat of reaction, kJ/mol

ε porosity of catalyst

ε_B bed voidage

$\varepsilon_l, \varepsilon_d, \varepsilon_s$ liquid holdup, total, dynamic and stagnant

η_c overall catalytic effectiveness factor

η_d, η_s, η_g catalytic effectiveness factors for dynamic, stagnant and dry zones

θ dimensionless temperature

θ_b dimensionless bed temperature

θ_W dimensionless wall temperature

μ_l viscosity of liquid, Pa.s

ρ_l density of liquid, kg/m^3

ρ_g density of gas, kg/m^3

ρ_p density of catalyst particle, kg/m^3

σ_l surface tension, N/m

τ tortuosity factor

ϕ Thiele parameter

Subscripts

d dynamic zone

g dry zone

s stagnant zone

Literature Cited

Al-Dahhan M. H. and M. P. Dudukovic, "Catalyst Bed Dilution for improving catalyst wetting in laboratory trickle bed reactors", *AIChE J.*, **42**, (9), 2595 (1996).

Al-Dahhan M.H., F.Larachi, M.P. Dudukovic and Laurent A., High-pressure trickle-bed reactors: A review, *Ind. Eng. Chem. Res.*, **36**, P.3292 (1997)

Dudukovic M. P., F Larachi and P. L Mills, Multiphase reactors – revisited, *Chem. Eng. Sci.*, **54**, 1975 (1999)

Baldi, G. in "Multiphase Chemical Reactors, Vol. II Design Methods", eds, A. E. Rodrigues, J. M. Cole and N. M. Sweed, p. 307. Sithoff and Noorldhoff, USA (1981)

Benaissa, M., G. C Le Roux,., X.Joulia, , R. V.Chaudhari., and H. Delmas,"Kinetic modeling of the hydrogenation of the hydrogenation of 1,5,9-Cyclododecatriene on Pd/Al_2O_3 catalyst including isomerization. *Ind. Eng. Chem. Res*., **35**, 2091-2095 (1996)

Bergault, I., M. V. Rajashekharam, R. V. Chaudhari, D. Schweich and H. Delmas "Modelling of comparison of acetophenone hydrogenation in trickle-bed and slurry airlift reactors" *Chem. Eng. Sci*., **52**, 21/22, 4033 (1997)

Barhme P.H., R.V Chaudhari., P.A Ramachandran.," Modelling of hydrogenation of glucose in a continuous slurry reactor". *Ind. Eng. Chem. Proc. Des. Dev*., **23**, 857 (1984)

Bischoff, K.B. 'Effectiveness factors for general reaction rate forms, *AIChE J*., **11**, 351 (1965)

Dassori C.G., "Three phase reactor modeling with significant back mixing in the liquid phase using modified cell model (MCM)", *Chem. Eng. Sci*., **22** (Suppl.), S679 (1998)

Fukushima, S., and K. Kusaka, " Liquid-phase volumetric mass transfer Coefficient and boundary of hydrodynamics flow regime in packed column with co current downward flow". *J. Chem. Eng. Japan*, **10**, 468 (1977)

Goto S., K. Mabuchi, "Oxidation of ethanol in gas-liquid cocurrent up-flow and downflow reactors", *Can. J. Chem. Eng*., **62**, 865 (1984)

Hanika, J., K. Sporka, V. Ruzicka, and R. Pistek, "Dynamic Behaviour of an Adiabatic Trickle Bed Reactor", *Chem. Eng. Sci*., **32**, 525 (1977)

Herrmann U. and G. Emig, "Liquid phase hydrogenation of maleic anhydride to 1-4, butanediol in a packed bubble column reactor", *Ind. Eng. Chem. Res*., **37**, 759 (1998)

Hochman, J. M. and Effron, E. "Two phase cocurrent downflow in packed Beds". *Ind. Eng. Chem. Fundam.,* **8,** 63 (1969)

Jaganathan R., Gholap R.V., Brahme P.H. and Chaudhari R.V, "Performance of a continuous bubble column slurry reactor for hydrogenation of butynediol.*Proceedings of ICREC 2*, NCL, India **II** 141 (1987)

Jaganathan, R., V.G. Ghugikar, R.V. Gholap, R.V. Chaudjari and P.L. Mills, 'Catalytic Hydrogenation of p-Nitrocumene in a Slurry Reactor', *Ind. Eng. Chem. Res.* **38**, 4634 (1999)

Julcour, C., R. Jaganathan, R.V. Chaudhari, A.M. Wilhelm and H. Delmas, "Selective Hydrogenation of 1,5,9-cyclododecatrien in up-flow and down flow fixed bed reactors, experimental observations and modeling" (Presented at ISCRE-16) *Chem. Eng, Sci.* (in press) (2000)

Khadilkar, M.R., Y.X. Wu, M. H. Al-Dahhan and M.P. Dudukovic, "Comparison of trickle bed and upflow reactor performance at high pressure: Model prediction and experimental observations", *Chem. Eng. Sci.,* **51** (10) 2139 (1996)

Khadilkar, M. R., Y. Jiang, M. Al-Dahhan, M. P. Dudukovic, S. K. Chou, G. Ahmed and R. Kahney, "Investigations of a complex reaction network: I Experiments in a high-pressure trickle bed reactor", *AIChE J.*, **44 (**4), 912 (1998)

Leung P., Zorrillla C., Recasens, Smith J.M., Hydration of isobutene in liquid-full and trickle bed reactors, *AIChE J.,* **32** (11), 1839 (1986)

Mills, P. L., Beaudry, E. G. And Dudukovic, M. P., Comparison and prediction of reactor performance for packed beds with two-phase flow : downflow, upflow and countercurrent flow. *I. Chem. E. Symp. Ser*., **87**, 527 (1984)

Mills, P. L. And Dudukovic, M. P. Evaluation of liquid-solid contacting in trickle bed reactors by tracer methods. *AIChE J*., **27**, 893 (1981)

Mills P.L. and R.V. Chaudhari, "Multiphase Catalytic Reactor Engineering and design for Pharmaceuticals and Fine Chemicals", *Cat. Today*, **37**, 367 (1997)

Mochizuki S. and T. Matsui, "Selective hydrogenation and mass transfer in a fixed bed catalytic reactor with gas-liquid concurrent upflow", AIChE J, **22**, (5) 904 (1976)

Ragaini V. and C. Tine, Upflow reactor for the selective hydrogenation of pyrolysis gasoline : Comparative study with respect to down flow, *Appl. Catal.,* **10**, 43 (1984)

Rajashekharam M. V., R. Jaganathan and R. V. Chaudhari, "A trickle-bed reactor model for hydrogenation of 2,4 dinitrotoluene: experimental verification". *Chem. Eng. Sci*., **53**, (4) 787 (1998)

Ramachandran P.A. and R.V. Chaudhari, "Three phase catalytic reactors", Gorden breach science publishers, New York, (1983)

Reiss, L. P. Cocurrent gas-liquid contacting in packed columns. *Ind. Eng. Chem. Proc. Des. Dev.,* **6**, 486 (1967)

Sato, Y., Hiros, T., Takahashi, F. and Toda, M. Pressure loss and liquid holdup in packed bed reactor with cocurrent gas-liquid flow. *J. Chem. Engng Japan,* **6**, 147 (1973)

Satterfield, C. N., Vab Eek, M. W. and Bliss, G. S. Liquid-Solid mass transfer in packed beds with down flow cocurrent gas-liqud flow. *AIChE J*., **24** (4), 709 (1978)

Specchia, V., Baldi, G., and Gianetto, A. Solid-liquid mass transfer in cocurrent two-phase flow through packed beds. *Ind. Eng. Chem. Proc. Des. Dev.,* **17**, 362 (1978)

Steigel, G. J., and Shah, Y. T. Backmixing and liquid holdup in gas-liquid cocurrent upflow packed column. *Ind. Eng. Chem. Proc. Des. Dev.,* **16**, 37 (1977)

Stephen, H and Stephen. I. Solubilities of Inorganic and Organic Compounds, Part -1, Vol. 1, p-543, Pergamon Press, UK (1963)

Stuber F., M. Benaissa and H. Delmas,"Partial hydrogenation of 1,5,9-cyclododecatriene in three phase catalytic reactors", *Catalysis Today,* **24**, 95 (1995)

Trambouze P., "Multiphase catalytic reactors in the oil industry: an introduction, *Rev. Inst. Fr. Pet*., **46**, 433 (1991)

Turpin, J. L., and Huntington, R. L. Prediction of pressure drop for two phase, two component cocurrent flow in packed beds. *AIChE J.,* **13**, 1196 (1967)

Van Gelder, K.B., J.K. Damhof, P.J. Krouenga and K.R. Westertrep,"Three phase packed bed reactor with an evaporating solvent I: Experimental: The hydrogenation of 2,4,6 - trinitrotoluene in methanol ", *Chem. Eng. Sci.*, **45**, 3159 (1990)

Van Gelder, K.B., P.C. Borman, R.E. Weenink, and K.R. Westertrep, Three phase packed bed reactor with an evaporating solvent II: Modelling the reactor, *Chem. Eng. Sci.*, **45**, 3171 (1990)

Wind, et. al. Upflow versus downflow testing of hydrotreating catalysts. *Applied Catalysis,* **43**, 239 (1988)

Wilke, C. R., and Chang, P. Correlation of diffusion coefficients in dilute solutions. *AIChE J.,* **1**, 264 (1955)

Yuanxin Wu, M. R khadilkar, M. H. Al-Dahhan, and M. P. Dudukovic, Comparison of upflow and downflow two-pahse flow packed bed reactors with and without fines : Experimental observation, *Ind. Chem. Eng. Res.,* **35**, 397 (1996)

Table 1. Experimental Work for Trickle bed (downflow) and Upflow Modes

Reaction System	Important Observations	Reference
Hydrogenation of α-methylstyrene	(a) In the low interaction regime trickle bed gave higher conversions than upflow. (b) Under conditions of liquid-phase reactant limitation, the upflow reactor is superior. When bed diluted by fines, both reactors perform identically under conditions of both gas- and liquid-phase limitations.	Mills et al. (1984), Wu et al. (1996), Khadilkar et al. (1996)
Hydrogenation of diolefin compounds	For better catalyst life and cycle efficiency, upflow reactor is preferable due to effective heat control.	Ragaini and Tine (1984)
Oxidation of ethanol	The reaction rates in both reactors were identical in the range studied. However, at lower liquid velocities the rates in trickle-bed reactor are higher.	Goto et al. (1984)
Hydration of isobutene	Reaction rates were higher in upflow reactor	Leung et al.(1986)
Performance of hydro treating catalysts	Upflow operation gave better utilization of the catalyst	de Wind et al. (1988)
Hydrogenation of butadiene	Selectivity better in upflow reactor compared to downflow	Vergel et al.(1993)
Hydrogenation of 1,5,9-cyclododecatriene	Rate of hydrogenation was higher in the upflow mode compared to downflow	Julcour et al. (2000)

Table 2. Kinetic parameters

Temperature (K)	$k_1 \times 10^2$ (m^3/kg)(m^3 /kmol/s)	$k_2 \times 10^2$ (m^3/kg)(m^3 /kmol/s)	$k_3 \times 10^2$ (m^3/kg)(m^3 /kmol/s)	K_B (m^3/kmol)	K_C (m^3/kmol)	K_E (m^3/kmol)
333	1.480	0.488	0.384	5.101	2.472	2.399
353	3.465	1.123	0.899	2.198	1.049	0.978
373	7.415	2.401	1.921	1.021	0.440	0.482
393	14.61	4.750	3.809	0.521	0.252	0.209

Table 3. Dimensionless Parameters Used in the Model

Mass transfer parameters

Gas-liquid mass transfer $\alpha_{gl} = k_l a_B L / U_l$

Liquid-solid mass transfer $\alpha_{ls} = k_s a_p L / U_l$

Gas-solid mass transfer $\alpha_{gs} = k_{gs} a_p L / U_l$

Nusslet number in dynamic zone $N_d = Rk_{s_d} / 3D_e$

Nusslet number in stagnant zone $N_s = Rk_{s_s} / 3D_e$

Nusslet number in dry zone $N_g = Rk_{gs} / 3D_e$

Thiele parameter

$$\phi = R / 3(\rho_p k_l B_{l_i} / D_e)^{0.5} \left[\frac{b_l + k_{21} c_l + k_{31} e_l}{1 + k_b b_l + k_c c_l + k_e e_l} \right]^{0.5}$$

Exchange parameter for stagnant zone

$$\alpha_s = (k_{ex} \varepsilon_{l_s} / f_s k_{s_s} a_p)$$

Heat transfer parameters

Thermicity parameter $\beta_l = \dfrac{(-\Delta H) B_{l_i}}{T_o C_{p_l} \rho_l (1 + [U_g C_{p_g} \rho_g / U_l C_{p_l} \rho_l])}$

Bed-to-wall heat transfer $\beta_2 = \dfrac{4 U_w L}{d_T C_{p_l} \rho_l (1 + [U_g C_{p_g} \rho_g / U_l C_{p_l} \rho_l])}$

Reaction rate & equilibrium constants

$\alpha_r = Lwk_l B_{l_i} / U_l$

$k_{21} = k_2 / k_1 ; k_{31} = k_3 / k_1$

$k_b = K_B B_{l_i} ; k_c = K_C B_{l_i} ; k_e = K_E B_{l_i}$

Table 4. Correlations Used for Downflow Modeling

Parameter	Correlation	Reference
Gas-liquid mass transfer coefficient	$\frac{k_l a_B d_p}{D(1-\varepsilon_l/\varepsilon_B)} = 2\left(\frac{S_p}{{d_p}^2}\right)^{0.2} {Re_l}^{0.73} {Re_g}^{0.2}\left(\frac{\mu_l}{\rho_l D}\right)^{0.5}\left(\frac{d_p}{d_T}\right)^{0.2}$	Fukushima and Kusaka (1977)
Liquid-solid mass transfer coefficient	$\frac{k_s d_p}{D}\frac{a_W}{a_p} = 0.815 Re_l^{0.822}\left(\frac{\mu_l}{\rho_l D}\right)^{0.333}$	Satterfield et al. (1978)
Volumetric mass exchange coefficient	$k_{ex} = 0.01 Re_l^{0.6}$	Hochmann and Effron (1969)
Total liquid holdup	$\frac{\varepsilon_l}{\varepsilon_B} = 0.185 {a_t}^{1/3} \chi^{0.22}$	Sato et al. (1973)
Bed-to-wall heat transfer coefficient	$\frac{U_W d_p}{\lambda_l} = 0.057\left(\frac{Re_l}{\varepsilon_l}\right)^{0.09} {Pr_l}^{1/3}$	Baldi (1981)
Wetting efficiency	$f_w = 1.104 {Re_l}^{1/3}\left[\frac{1+[(\Delta P/Z)/\rho_l g]}{Ga_l}\right]^{1/9}$	Al-Dahhan et al. (1995)

Table 5. Correlations Used for Upflow Modeling

Parameter	Correlation	Reference
Gas-liquid mass transfer coefficient, $k_l a_B$	$k_l a_B = 5.48 \times 10^{-3} \left[U_l \delta_{gl} \right]^{0.5}$	Reiss (1967)
Pressure drop per unit length of reactor, δ_{gl}	$\left[\delta_{gl} \right]^{0.5} = \frac{2 f_{gl} U_g^2 \rho_g}{d_{pe}}$	Turpin and Huntington (1967)
Liquid-solid mass transfer coefficient, k_s	$k_s = \left(0.48 \ln\left(\frac{Re_g 10^2}{Re_l} \right) - 0.03 \left(\ln\left(\frac{Re_g 10^2}{Re_l} \right) \right)^2 - 0.3 \right) \frac{D_{12} Sh_0}{d_p}$	Specchia et al. (1978)
Liquid hold up, ε_l	$\varepsilon_l = \varepsilon_B 1.47 Re_l^{0.11} Re_g^{-0.19} \left(a_p d_p \right)^{-0.41}$	Stiegel and Shah (1977)

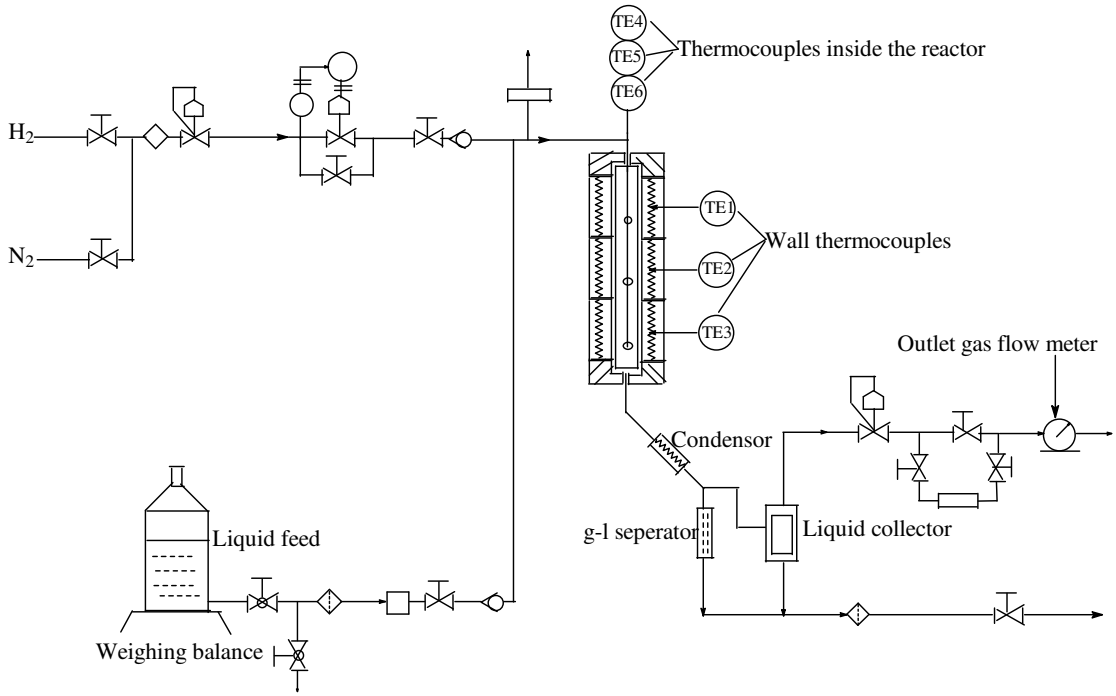

Figure 1. Reactor setup.

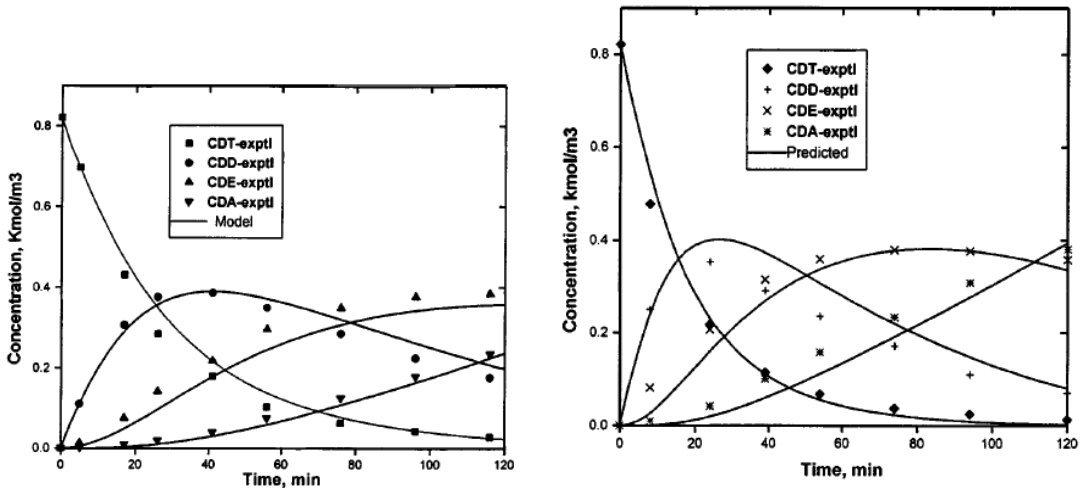

Figure 2. Concentration-time profiles in a batch slurry reactor for (a) 353 K and (b) 373 K

Reaction conditions: iInitial concentration of CDT: 0.82 kmol/m^3; pressure: 1.2 MPa; catalyst Loading: 1.82 kg/m^3; agitation speed: 1100 rpm

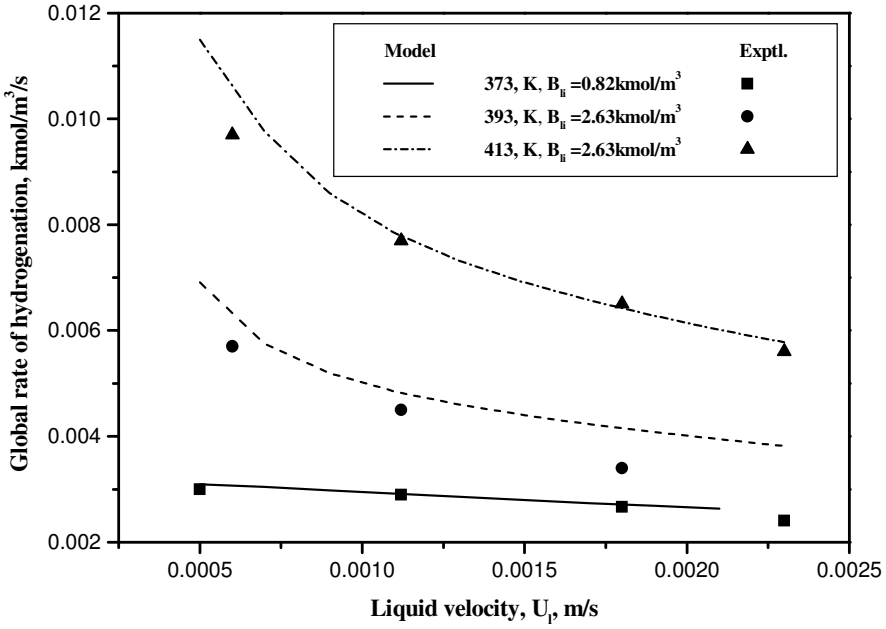

Figure 3. Effect of liquid velocity on global rate of hydrogenation in trickle bed (downflow) for different inlet temperatures

Reaction conditions: P_H = 1.2 MPa; U_g = 3.9 x10^{-3} m/s

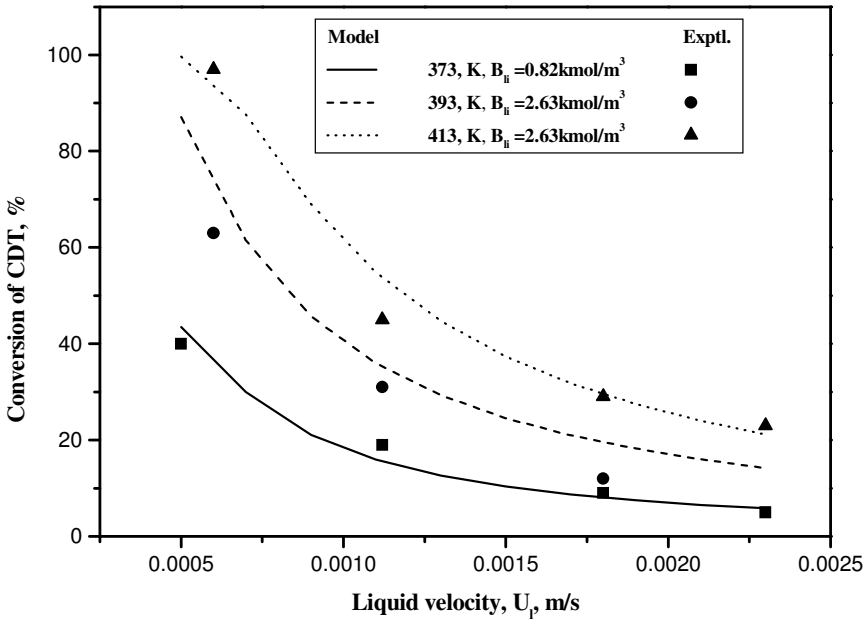

Figure 4. Effect of liquid velocity on conversion of CDT in trickle bed (downflow) at different inlet temperatures

Reaction conditions: P_H = 1.2 MPa; U_g = 3.9 x10^{-3} m/s

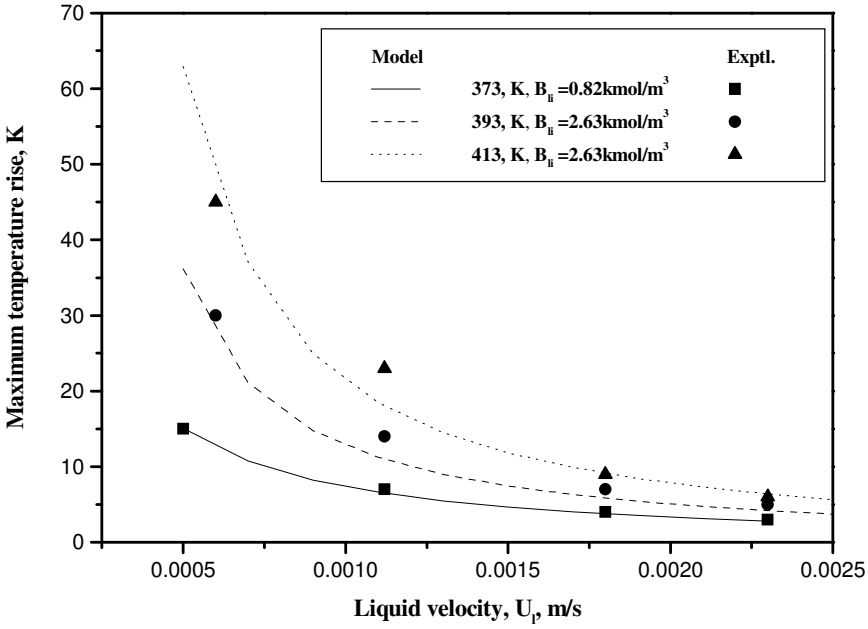

Figure 5. Effect of liquid velocity on maximum temperature rise (ΔT) in trickle bed (downflow) at different inlet temperatures.

Reaction conditions: inlet CDT = 0.82 kmol/m^3; P_H = 1.2 MPa; U_g =3.9 x10^{-3} m/s

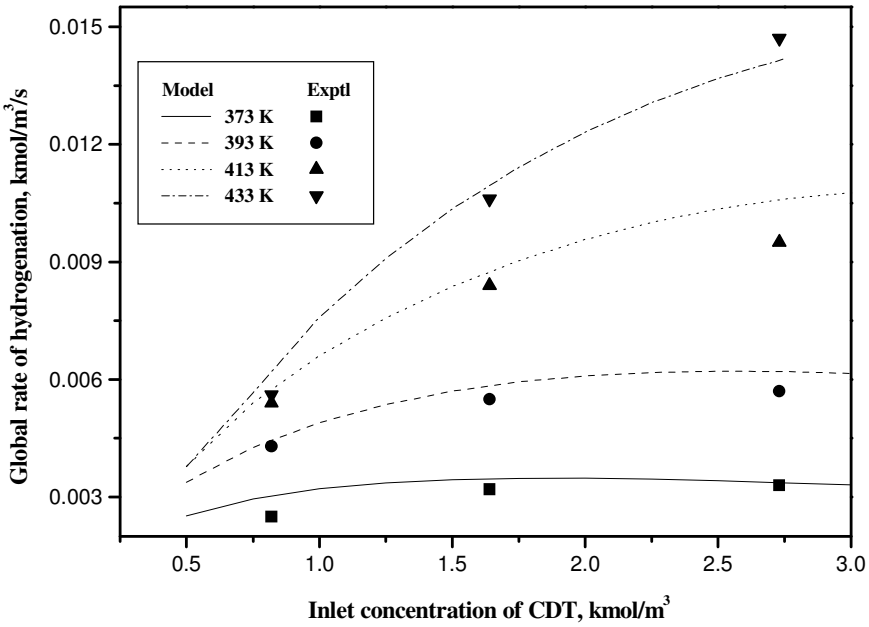

Figure 6. Effect of inlet CDT concentration on global rate of hydrogenation in trickle bed reactor (downflow)

Reaction conditions: P_H = 1.2 MPa; U_l = 1.2 x10^{-3} m/s; U_g = 3.9 x10^{-3} m/s

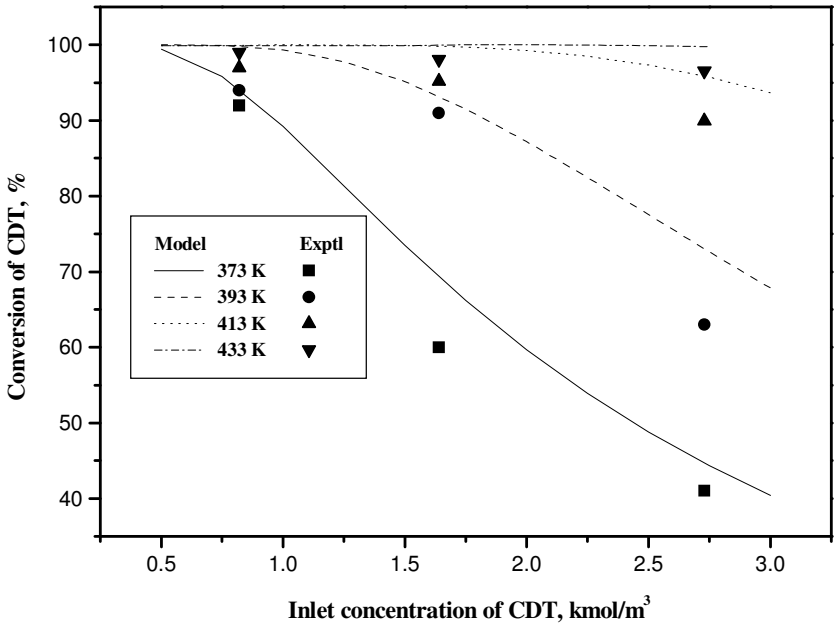

Figure 7. Effect of inlet CDT concentration on conversion of CDT in trickle-bed reactor (downflow)

Reaction conditions: P_H = 1.2 MPa; U_l = 1.2 x10^{-3} m/s; U_g = 3.9 x10^{-3} m/s

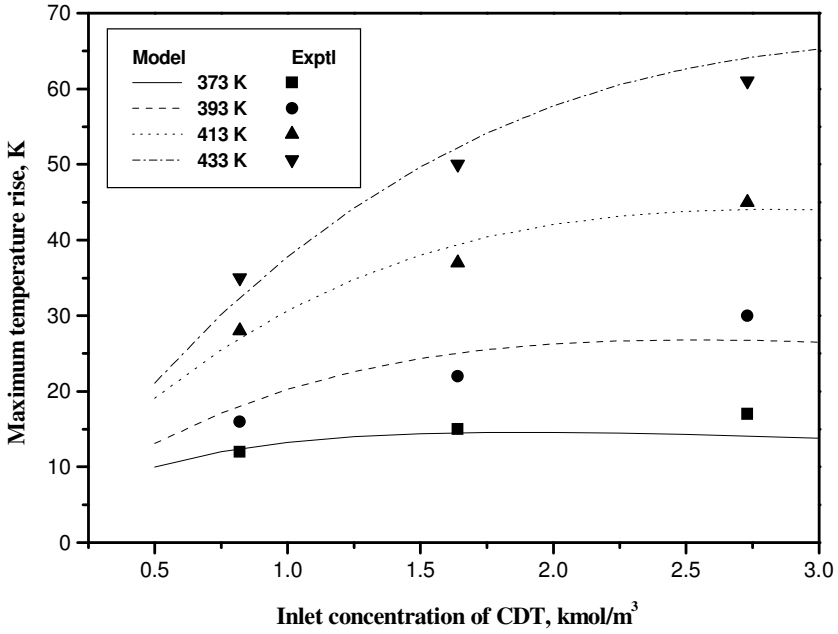

Figure 8. Effect of inlet CDT concentration on maximum temperature rise (ΔT) in a trickle-bed reactor (downflow)

Reaction conditions: P_H = 1.2 MPa; U_l = 1.2 x10^{-3} m/s; U_g = 3.9 x10^{-3} m/s

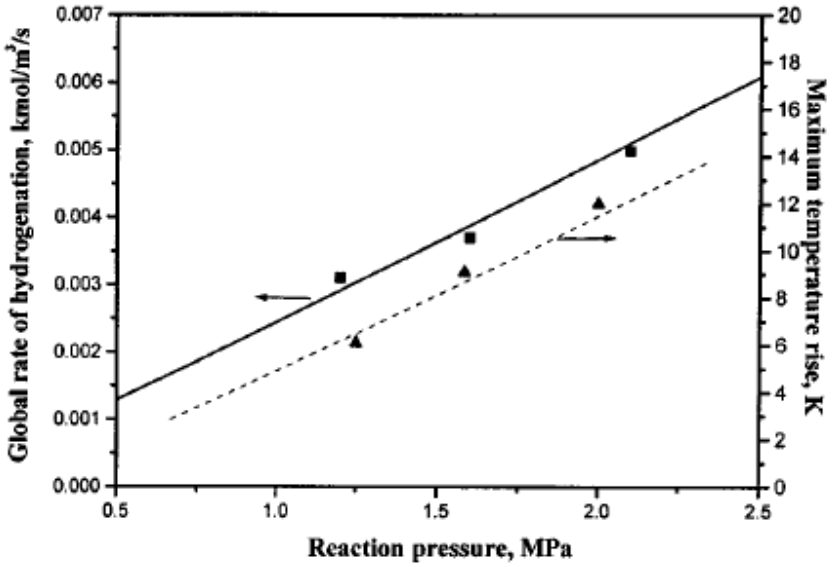

Figure 9. Effect of hydrogen pressure on global rate and temperature rise in a trickle bed (downflow)

Reaction conditions: T = 373 K; Inlet CDT = 0.82 kmol/m^3; U_l = 1.2 x10^{-3} m/s; U_g = 3.9 x10^{-3} m/s

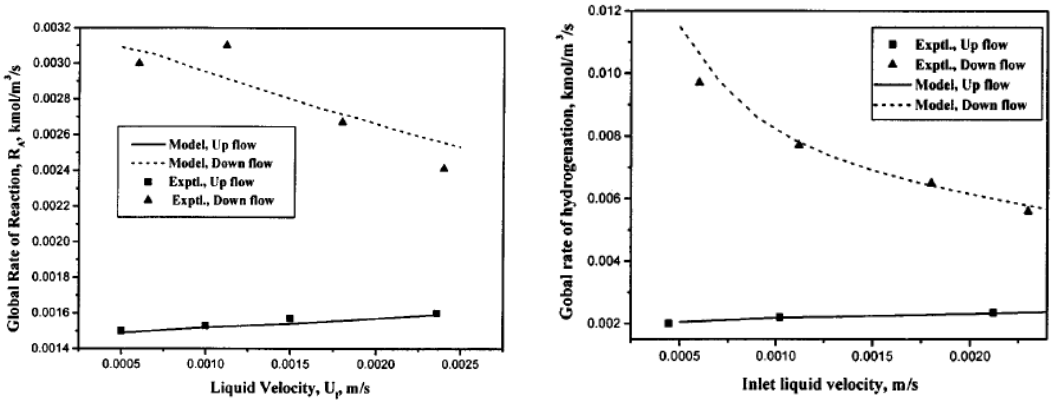

(a) **(b)**

Figure 10. Effect of liquid velocity on global rate of hydrogenation in trickle bed and upflow modes.

Reaction conditions: P_H = 1.2 MPa; U_g = 3.9 x10^{-3} m/s

(a) T = 373 K, inlet CDT = 0.82 kmol/m^3;

(b) T = 413 K, inlet CDT = 2.63 kmol/m^3;

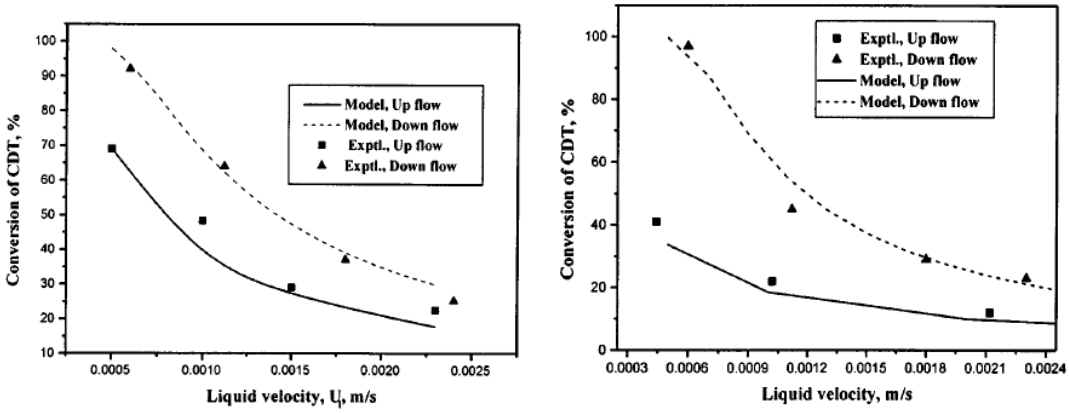

(a) **(b)**

Figure 11. Effect of liquid velocity on conversion of CDT in trickle bed and upflow modes.

Reaction conditions: P_H = 1.2 MPa; U_g = 3.9 x10^{-3} m/s

(a) T = 373 K, inlet CDT = 0.82 kmol/m^3;

(b) T = 413 K, inlet CDT = 2.63 kmol/m^3;

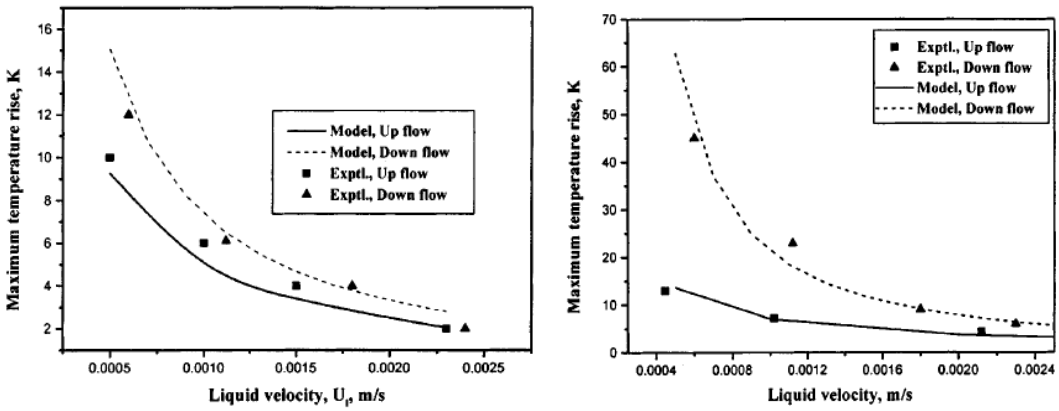

(a) **(b)**

Figure 12. Effect of liquid velocity on temperature rise in trickle bed and upflow modes.

Reaction conditions: P_H = 1.2 MPa; U_g = 3.9 x10^{-3} m/s

(a) T = 373 K, inlet CDT = 0.82 kmol/m^3;

(b) T = 413 K, inlet CDT = 2.63 kmol/m^3;

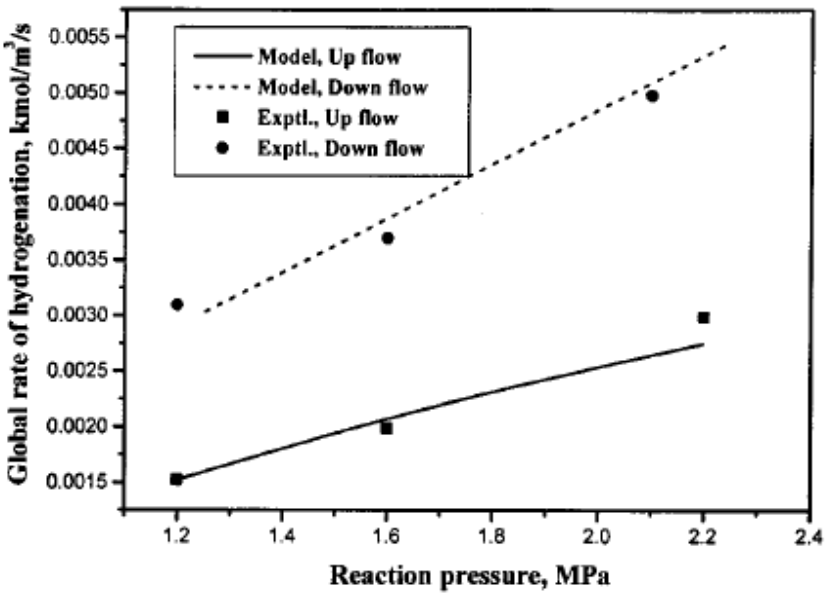

Figure 13. Effect of hydrogen pressure on global rate of hydrogenation in trickle bed and upflow modes.

Reaction conditions: T = 373 K; inlet CDT = 0.82 kmol/m^3; U_l = 1.2 x10^{-3} m/s; U_g = 3.9 x10^{-3} m/s

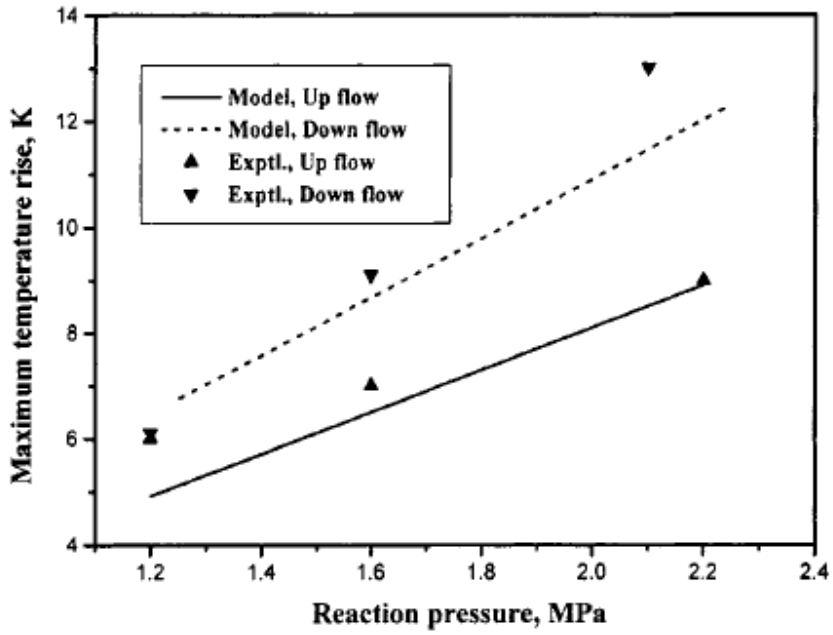

Figure 14. Effect of hydrogen pressure on temperature rise in trickle bed and upflow modes.

Reaction conditions: T = 373 K; inlet CDT = 0.82 kmol/m^3; U_l = 1.2 x10^{-3} m/s; U_g = 3.9 x10^{-3} m/s

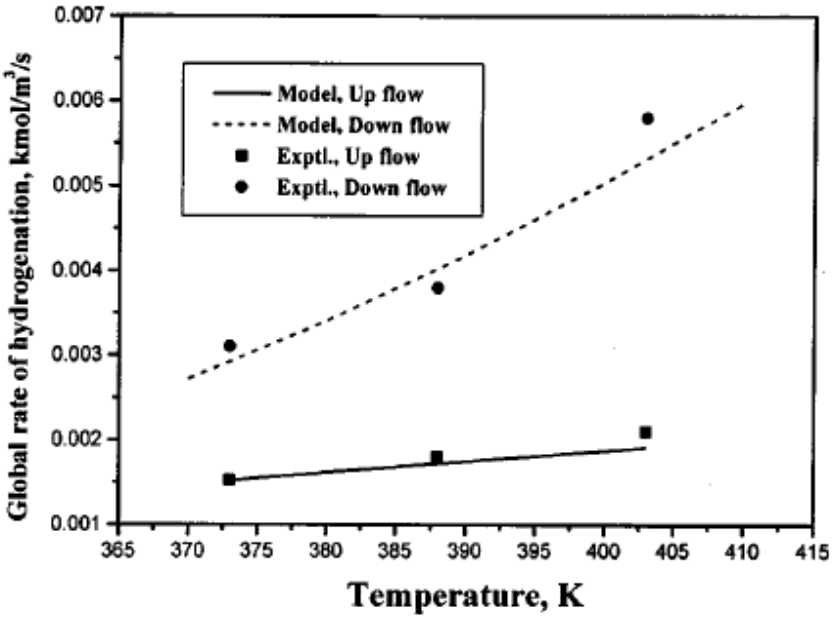

Figure 15. Effect of inlet temperature on global rate of hydrogenation in trickle bed and upflow modes.

Reaction conditions: inlet CDT = 0.82 kmol/m^3; P_H = 1.2 MPa; U_l = 1.2 x10^{-3} m/s; U_g = 3.9 x10^{-3} m/s

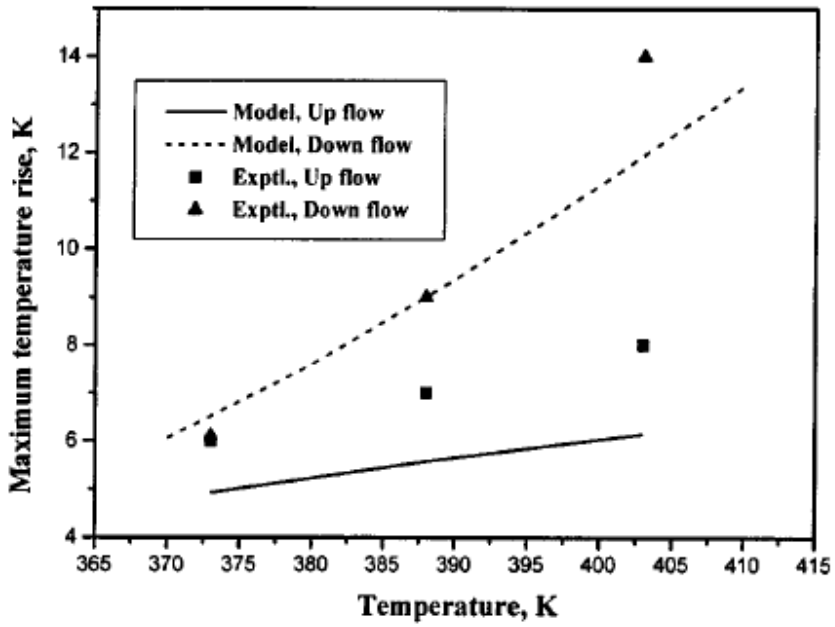

Figure 16. Effect of inlet temperature on temperature rise in trickle bed and upflow modes.

Reaction conditions: inlet CDT = 0.82 kmol/m^3; P_H = 1.2 MPa; U_l = 1.2 x10^{-3} m/s; U_g = 3.9 x10^{-3} m/s

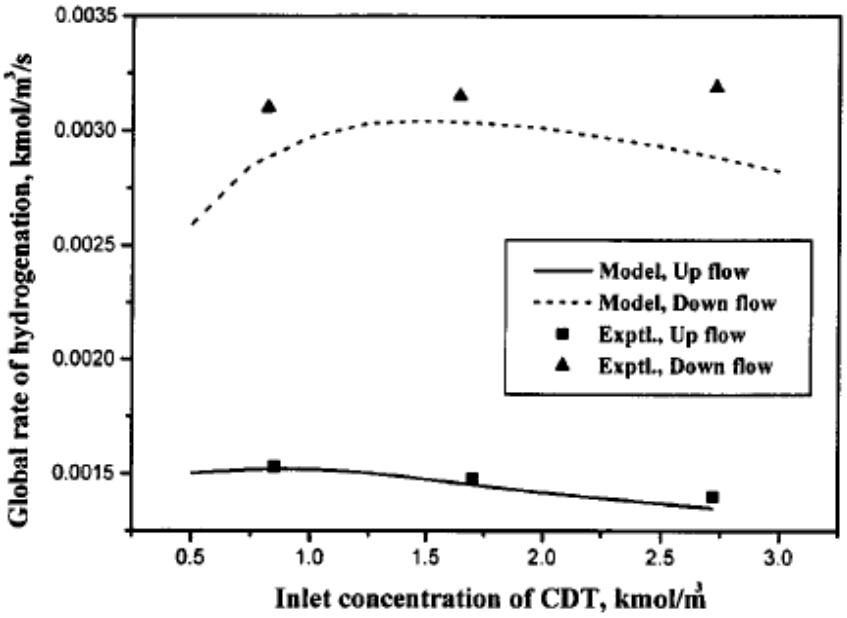

Figure 17. Effect of inlet CDT concentration on global rate of hydrogenation In trickle bed and upflow modes.

Reaction conditions: T = 373 K; P_H = 1.2 MPa; U_l = 1.2 x10^{-3} m/s; U_g = 3.9 x10^{-3} m/s

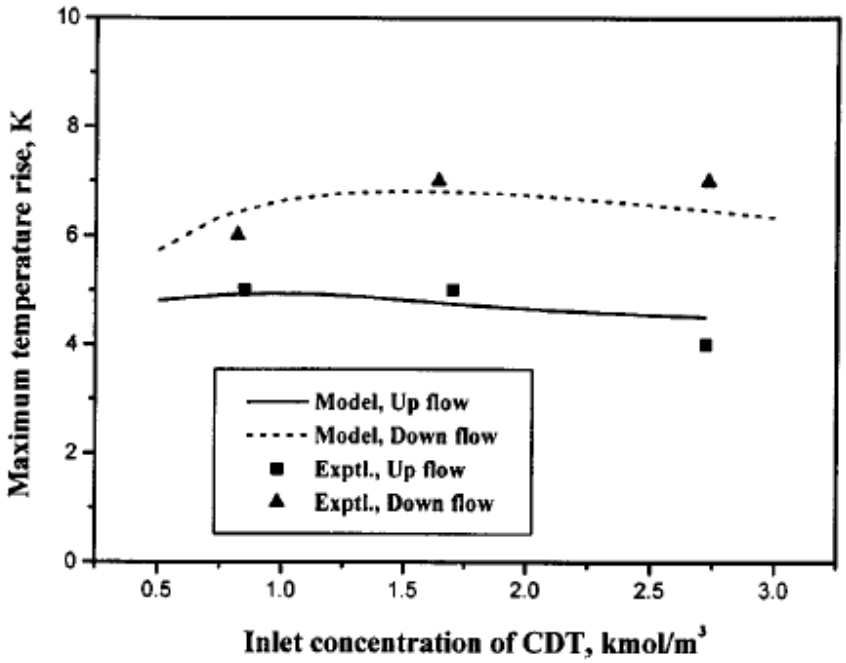

Figure 18. Effect of inlet CDT concentration on temperature rise in upflow and downflow reactors.

Reaction conditions: T = 373 K; P_H = 1.2 MPa; U_l = 1.2 x10^{-3} m/s; U_g = 3.9 x10^{-3} m/s

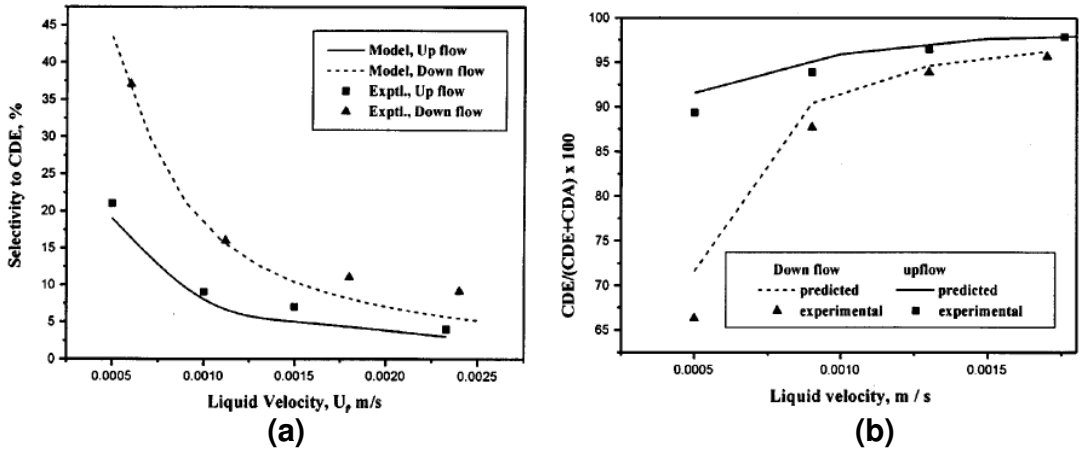

Figure 19. Effect of U_l on selectivity for upflow and downflow reactors.

Reaction conditions: T = 373 K; inlet CDT = 0.82 kmol/m^3; P_H = 1.2 MPa;

$U_g = 3.9 \times 10^{-3}$ m/s

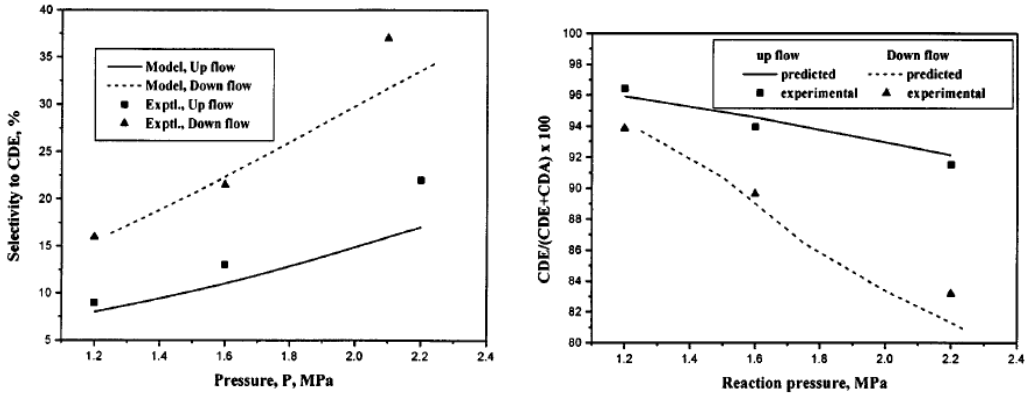

(a) **(b)**

Figure 20. Effect of Pressure on selectivity for upflow and downflow reactors.

Reaction conditions: T = 373 K; inlet CDT = 0.82 kmol/m^3; U_l = 1.2 x10^{-3} m/s; U_g = 3.9 x10^{-3} m/s

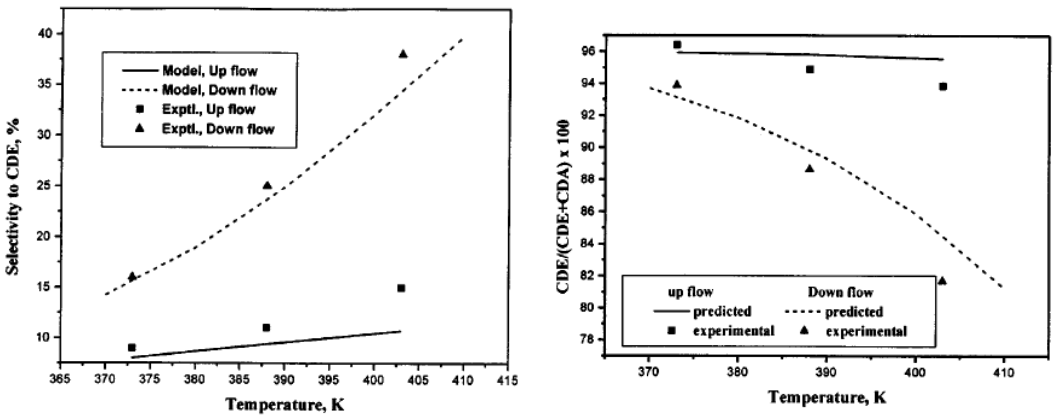

Figure 21. Effect of inlet temperature on selectivity of CDE for upflow and downflow reactors.

Reaction conditions: inlet CDT = 0.82 kmol/m^3; P_H = 1.2 MPa; U_l = 1.2 x10^{-3} m/s; U_g = 3.9 x10^{-3} m/s

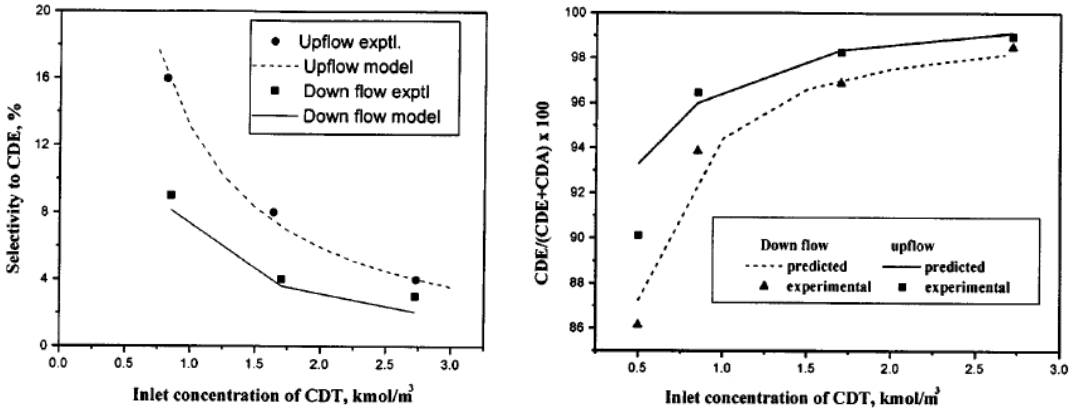

(a) **(b)**

Figure 22. Effect of inlet CDT concentration on selectivity of CDE for up-flow and downflow reactors.

Reaction conditions: T = 373 K; P_H = 1.2 MPa; U_l = 1.2 x10^{-3} m/s; U_g = 3.9 x10^{-3} m/s